Published in final edited form as:
Tetrahedron. 2013 September 9; 69(36): 7741–7746. doi:10.1016/j.tet.2013.05.092.

A noncovalent, fluoroalkyl coating monomer for phosphonate-covered nanoparticles

Vincent Li[a], **Andy Y. Chang**[b], and **Travis J. Williams**[a,*]

[a]Loker Hydrocarbon Research Institute, Department of Chemistry, University of Southern California, 837 Bloom Walk, Los Angeles, CA 90089-1661, USA

[b]The Saban Research Institute of Children's Hospital of Los Angeles, 4650 Sunset Boulevard, Los Angeles, CA 90027-6062, USA

Abstract

Gadolinium-containing phosphonate-coated gold nanoparticles were prepared and then non-covalently coated with an amphiphilic fluorous monomer. The monomer spontaneously self-assembles into a non-covalent monolayer shell around the particle. The binding of the shell utilizes a guanidinium-phosphonate interaction analogous to the one exploited by the Wender molecular transporter system. Particle-shell binding was characterized by a 27% decrease in ^{19}F T_1 of the fluorous shell upon exposure to the paramagnetic gadolinium in the particle and a corresponding increase in hydrodynamic diameter from 3 nm to 4 nm. Interestingly, a much smaller modulation of ^{19}F T_1 is observed when the shell monomer is treated with a phosphonate-free particle. By contrast, the phosphonate-free particle is a much more relaxive ^{1}H T_1 agent for water. Together, these observations show that the fluoroalkylguanidinium shell binds selectively to the phosphonate-covered particle. The system's relaxivity and selectivity give it potential for use in ^{19}F based nanotheranostic agents.

Keywords

Theranostic; Gold nanoparticle; Surfaces; Relaxivity; Fluorine

1. Introduction

The development of "smart" nanoparticulate medicinal entities is an emerging area at the interface of chemical and clinical sciences. For example, novel drug delivery systems and imaging agents based on drug-loaded polymers or nanoparticles have appeared recently,[1] and are making way into the clinic.[2] Nanotechnology further offers opportunities to design combined therapeutic plus diagnostic agents, or "theranostic" systems; examples of such include paramagnetic nanoparticles for MRI imaging,[3] ^{64}Cu-loaded liposomes for PET imaging,[4] and others.[5]

*Corresponding author. Tel.: +1-213-740-5961; fax: +1-213-740-6679; travisw@usc.edu.

Dedication

To Paul Wender, who taught us as undergraduate (AYC) and graduate (TJW) students to "suspend the constraints of reality."

Supplementary Material

Graphical 1-D and 2-D NMR spectra, NMR T_1 inversion recovery spectra and fits, optical absorption spectra, and DLS histograms. Supplementary data associated with this article can be found in the online version, at http://dx.doi.org/xxx

One key factor to controlling the in vivo behavior of these systems is the ability to control their surface properties.[6] Along these lines, we are pursuing the development of monomeric organic compounds that engage in predictable self-assembly around nanoparticulate molecular probes and that have the ability to control the bioactivity of the former by modifying their size, surface, and access to the external aqueous milieu.[7]

We present here a general strategy for applying a poly)ethyleneglycol (PEG)-terminated fluoroalkyl coating to phosphonate-covered nanoparticle agent and illustrate the use of bioorthogonal ^{19}F magnetic resonance relaxivity to track the behavior of the coating monomer as it associates with the particle. The coating monomer (**1**, Fig. 1) exploits a guanidinium head group, which can interact with particle surface phosphonate groups through a double hydrogen bonding system analogous to the one used by the Wender molecular transporter system for its initial adhesion to cell surfaces.[8] Particles utilizing such coreshell interactions have various clinical applications, such as vectors for gene delivery, as investigated in the Wender lab[9]. Monomer **1** further features a fluoroalkane region that enables the self-assembly of a fluorous, Teflon-like layer that can limit the particle's exposure to its aqueous surroundings.

We have previously characterized the binding of monomer **1** with small-molecule phosphonates,[10] and we hypothesize that a particle with a phosphonate surface can utilize the same interaction(s) to bind species **1**, thus enabling the self-assembly of a monolayer coating around a particle (Fig. 2). Incorporating a paramagnetic species into such a particle can thus enable the use of monomer **1** as a ^{19}F MRI contrast system for an appropriately filtered, T_1-weighted image plane. Although ^{19}F MRI-based nanotheranostic technology is not as well developed as the analogous ^{1}H MRI based systems, ^{19}F MRI based systems are beginning to emerge,[11,12] and offer important bioorthogonality unavailable to other imaging modalities.[13] We show here potential utility of monomer **1** as a flexible tool for the installation of ^{19}F groups on the surface of a phosphonatecovered nanoparticle and illustrate the corresponding modulation in ^{19}F T_1 upon particle-**1** binding. We further illustrate **1**'s selectivity for a phosphonate surface over a phosphonate free particle and illustrate that the coverage provided by **1** corresponds to a monolayer in aqueous solution.

2. Results and discussion

2.1. Design and synthesis of shell monomer 1

Shell monomer **1** features a guanidinium head group, which is designed to participate in hydrogen bonding with phosphonates on the periphery of a particle. This is attached to a fluorous phase group[14] that prevents intercalation of the shell in to the interior of the particle and limits the particle's exposure to its surroundings. Appropriate fluorous starting materials for this design are readily available side products from teflon synthesis.[15] A hydrophilic PEG chain is then appended as a solubilizing group. Scheme 1 summarizes the synthesis of monomer **1**, which we have previously reported.[10] This route relies on the intermediacy of a bench top-stable alkyl triflate (**4**), which is a versatile starting material for fluoroalkyl amines.

2.2. NMR properties of monomer 1

Shell monomer **1** exhibits 3 different peaks in the ^{19}F NMR spectrum, which can be rigorously assigned by a combination of ^{19}F-^{13}C HMBC and ^{13}C-^{1}H HSQC NMR spectra (see supporting information). The most downfield signal (−117.9 ppm, peak A) corresponds to the fluorine CF_2 group nearest the guanidine of **1**. An upfield (−123.5 ppm, peak C) multiplet corresponds to the two central CF_2 groups, and the middle peak of the ^{19}F spectrum (−119.8 ppm, peak B) corresponds to the fluorines closest to the PEG tail: see

Supporting Information regarding the ^{19}F signal assignments. The T_1 relaxation times were measured in 25 mM pH = 7.6 TRIS-HCl buffer and were found to be 457(8) ms, 436(7) ms, and 497(7) ms for peaks A, B, and C respectively. These data are summarized in Fig. 3

2.3. Design and synthesis of paramagnetic nanoparticles

Our design for a template nanoparticle is based on a very simple gold-centered structure, which is decorated with a periphery of thiol-terminated phosphonic acid surfactants (Fig. 4). The selection of this construction is based on its popularity in several scaffolds currently being developed for drug delivery and clinical imaging applications.[16] It enables concise size control and flexibility of surface functionalization.[17, 18] In this section we present synthetic routes for paramagnetic particles functionalized with both [Gd(DOTA)] and phosphonate peripheries.

A 1.5 nm phosphine-stabilized gold core (**10**) was first synthesized based on previously reported conditions.[19] Thiols **6** and **7** were assembled onto the gold core via interfacial ligand exchange in a biphasic water/dichloromethane system (Scheme 2A).[20] The resulting particles form visible aggregates at neutral pH, but are stable in a pH = 7.6 TRIS-HCl buffer. Monomer **1** spontaneously self assembles onto particles **8** immediately upon introduction to an aqueous solution of **8** to yield hybrid gadolinium-phosphonate particles **2**.

Phosphonate-free particles **9** are apparently unstable to aggregation when prepared according to the procedure above, but in-situ deprotection of trityl-protected thiol **11** followed by treatment with $HAuCl_4$ can be used to generate these particles (Scheme 2B).[21] This method yields particles that are of 7 nm in hydrodynamic diameter as measured by dynamic light scattering (DLS). ^{19}F longitudinal relaxivity time constants (^{19}F T_1) provide evidence for the binding of particle and monomer **1**. Upon binding of **1** to the particle core, the fluorine nuclei are brought into close proximity of the particle's paramagnetic gadolinium centers, where the paramagnetic gadolinium center causes a decrease in the T_1 relaxation times of the ^{19}F nuclei.[22]

2.4. Particle-shell binding

Upon addition of an aqueous solution of particle **8** to **1**, the ^{19}F T_1 relaxation times for **1** decreased to 332(14) ms, 348(4) ms and 385(4) ms respectively (Table 1). Significant decrease of the observed T_1 values upon the addition of paramagnetic particles is consistent with an intimate interaction between **1** and the particle core. To assess the role of the phosphonate functionality on particle **8**, phosphonate free particles **9** were also treated with **1**. In this experiment, the T_1 relaxation times were 434(6) ms, 431(7) ms, 481(5) ms. These data show that **9** exhibits lower changes in T_1 than those observed for particle **8**. This suggests a more intimate interaction between **1** and **8** versus **1** and **9**. Furthermore, exposure of the shell (**1**) to 1.0 mM $GdCl_3$ (0.25 molar equivalents relative to **1**, 158 ppm wt/wt [Gd]) also resulted in a less significant change in ^{19}F T_1 than our phosphonate coated particles (**8**, Table 1), which shows that high [Gd] alone can not account for the observed decrease in ^{19}F T_1 observed in the presence of **8**.

^{1}H T_1 time constants of H_2O for aqueous solutions of particles **8** and **9** reveal that, although **8** is a more effective ^{19}F T_1 contrast agent, **9** is a more efficient ^{1}H T_1 contrast agent. We measured the H_2O ^{1}H T_1 relaxation of the same particle solutions used for acquisition of the foregoing ^{19}F T_1 data. Particle **8** showed a ^{1}H T_1 of 1.18(5) s, and particle **9** exhibited a T_1 of 0.495(3) s. The significantly lower H_2O ^{1}H T_1 of **9** shows that it is a more relaxive ^{1}H contrast agent, whereas particle **8** is a more relaxive ^{19}F T_1 contrast agent. *This remarkable contrast between ^{1}H and ^{19}F highlights the importance of a guanidinium-phosphate interaction in binding **1** to the particles*: whereas phosphonaterich **8** holds **1** in the proximity

of the paramagnetic gadolinium, phosphonate-free **9** does so less well, relative to a water standard. Moreover, absolute gadolinium concentration measurements by ICP (ppm wt/wt) indicate [Gd] = 52 ppm in the experimental solution of **8** and [Gd] = 37 ppm in the experimental solution of **9**. Although these values are similar, they are inconsistent with the relatively short ^{1}H T_1 of the **9** solution, which can be attributed to slower tumbling of the larger particle.

2.5. Particle sizes

The foregoing relaxivity-based shell binding data are supported by dynamic light scattering (DLS) measurements. DLS data for particle **8** indicate monodisperse particles of hydrodynamic diameter of 3.0 nm (Fig. 5A). Addition of shell to the particle increased the size of the particle to 4.0 nm (Fig. 5B). The increase in diameter of 1 nm upon association of **1** is appropriate for the addition of two equivalents of **1**, along with associated water, along the diameter. Further, these data also show that the particles are not aggregating upon changing their surface from phosphonate to PEG.

3. Conclusion

In conclusion we have characterized the non-covalent coating of a gadolinium-containing gold nanoparticle with a fluorous shell. The coating utilizes a phosphonate-guanidine interaction and is characterized by both a decrease in ^{19}F T_1 and an appropriate increase in the particle's hydrodynamic radius. We further use ^{1}H and ^{19}F NMR relaxivity data to show that phosphonate groups on the surface of a particle increase the particle's affinity for fluoroguanidine **1** relative to water. Because these observations describe a general procedure for the selective self-assembly for fluoroaklyl groups around the surface of a phosphonate-covered material, we believe that they have potential applications in biomaterials and ^{19}F MRI-based nanotheranostic systems.

4. Experimental section

General procedures

Deuterated NMR solvents were purchased from Cambridge Isotopes Labs. All NMR spectra were obtained on a Varian 500 MHz spectrometer at 25 °C. DLS were acquired on a Wyatt Dynapro Titan instrument. UV-Vis spectra were acquired on a Shimadzu UV-1800 spectrometer. Phosphine-stabilized gold nanoparticles (**9**) with diameter 1.5 nm were synthesized according to previously reported conditions,[23] and characterized by a match of their UV-Vis spectrum. TRIS buffer was purchased from Angus Chemicals. ICP-MS data were acquired by the University of Illinois at Urbana-Champaign School of Chemical Sciences Microanalysis Laboratory.

4.1. Synthesis of gadolinium-thiol 6

Gadolinium thiol **6** was synthesized based on previously reported conditions.[23] Mass data for **6** is consistent with a known sample. MALDI for $C_{19}H_{32}GdN_5O_7S$: Calculated 632.13 g/mol; found 631.94 g/mol. Measured isotopic distribution matches calculated prediction.

4.2. Synthesis of particle 8

Phosphine stabilized gold nanoparticles **10** (1.0 mg) were dissolved in dichloromethane (1 mL), and TRIS-HCl buffer (1 mL of 25 mM pH = 7.6) was added to form a biphasic mixture. While stirring at room temperature, gadolinium thiol **6** (40 μL of a 10 mM aqueous solution) was added, and the solution was stirred for 4 hours. Thiol phosphonic acid **7**[24] was then added and the reaction was stirred until the brown color partitioned completely into the

aqueous layer. The aqueous layer was diluted with TRIS-HCl buffer (1.0 mL of a 25 mM solution at pH = 7.6) and extracted with dichloromethane[25] (5 mL, 5 times), then filtered through a 0.45 μm syringe filter to yield an aqueous solution of particle **8**.

4.3. Synthesis of particle 9

Trityl-protected gadolinium complex **11** (33.4 mg, 38 μmol) was suspended in tetrahydrofuran (0.4 mL). Chloroauric acid[26] ($HAuCl_4$, 13.0 mg, 38 μmol) was added to the solution at room temperature and the reaction was stirred for 1 hour. Triethyl silane[27] (Et_3SiH, 4.2 mg, 38 μmol) was then added, and the solution stirred for 18 hours at room temperature. The solution was filtered and ethanol[28] (10 mL) was added to initiate precipitatation. The precipitate was washed with ethanol (5 times, 10 mL), and the filter paper was sonicated in H_2O (10 mL) to dissolve precipitate. The resulting aqueous solution was then filtered through a 0.45 mm syringe filter to yield particles **9** as an aqueous solution. DLS measurements on the resulting solution showed a monodisperse nanoparticulate material with hydrodynamic diameter of 7 nm.

4.4. Measurement of ^{19}F T_1 of 1-coated particles

A portion of **1** (3 μL of a 100 mM solution) was lyophilized to an oil in a 1/2 dram glass vial. A 125 μL aliquot of aqueous particle solution was delivered to the vial containing lypholized **1**, stirred, then placed in a 3 mm diameter coaxial NMR tube insert and ^{19}F T_1 time constants were acquired using the parameters previously stated.

Supplementary Material

Refer to Web version on PubMed Central for supplementary material.

Acknowledgments

This work is sponsored by the Donald E. and Delia B. Baxter Foundation, the USC Ming Hsieh Institute, and the Robert E. and May R. Wright Foundation. We are grateful to the National Science Foundation (DBI-0821671, CHE-0840366), the National Institutes of Health (1 S10 RR25432), and the University of Southern California for their sponsorship of NMR spectrometers. We are grateful to Anna Dawsey for synthesis of the gold core, Xinping Wu for the synthesis of the shell monomer, Christopher Beier for assistance in acquiring UV-Vis spectra, Dr. Shuxing Li and the USC nanobiophysics core for assistance in acquiring DLS data, and Dr. Allan Kershaw for assistance in acquiring NMR data.

References and Notes

1. Barreto JA, O'Malley W, Kubeil M, Graham B, Stephan H, Spiccia L. Mat. Views. 2011; 23:H18.
2. (a) Gabizon A, Catane R, Uziely B, Kaufman B, Safra T, Cohen R, Martin F, Huang A, Barenholz Y. Cancer Res. 1994; 54:987. [PubMed: 8313389] (b) Lasic DD. Nature. 1996; 380:561. [PubMed: 8606781] (c) Malam Y, Loizidou M, Seifalian AM. Trends Pharmacol. Sci. 2009; 30:592. [PubMed: 19837467]
3. a) Xie J, Chen K, Huang J, Lee S, Wang J, Gao J, Li X, Chen X. Biomaterials. 2010; 31:3016. [PubMed: 20092887] b) Zhang F, Huang X, Zhu L, Guo N, Niu G, Swierczewska M, Lee S, Xu H, Wang AY, Mohamedali KA, Rosenblum MG, Lu G, Chen X. Biomaterials. 2012; 33:5414. [PubMed: 22560667] c) Medarova Z, Rashkovetsky L, Pantazopoulos P, Moore A. Cancer Res. 2009; 69:1182. [PubMed: 19141648] d) Guthi JS, Yang S, Huang G, Li S, Khemtong C, Kessinger CW, Peyton M, Minna JD, Brown KC, Gao J. Mol. Pharmaceutics. 2009; 7:32.
4. Peterson AL, Binderup T, Rasmussen P, Henriksen JR, Elma DR, Kjaer A, Andresen TL. Biomaterials. 2001; 32:2334.
5. Rowe MD, Thamm DH, Kraft SL, Boyes SG. Biomacromolecules. 2009; 10:983. [PubMed: 19290624]

6. a) Chen T, Xu S, Zhao T, Zhu L, Wei D, Li Y, Zhang H, Zhao C. ACS Appl. Mater. Interfaces. 2012; 4:5766. [PubMed: 23043448] b) Marega R, Karmani L, Flamant L, Nageswaran PG, Valembois V, Masereel B, Feron O, Borght TV, Lucas S, Michiels C, Gallez B, Bonifazi D. J. Mater. Chem. 2012; 22:21305.c) Bisker G, Yeheskely-Hayon D, Minai L, Yelin D. J. Controlled Release. 2012; 162:303.d) Bhattacharyya S, Khan JA, Curran GL, Robertson JD, Bhattacharyya R, Mukherjee P. Adv. Mater. 2011; 23:5034. [PubMed: 21971980] e) Giljohann DA, Seferos DS, Daniel WL, Massich MD, Patel PC, Mirkin CA. Angew. Chem. Int. Ed. 2010; 49:3280.
7. a) Chang, AY.; Williams, TJ.; Boz, E. Ultrasound-Activated Nanoparticles as Imaging Agnets and Drug Delivery Vehicles PCT. Int. Appl. WO2011079317 A3. 2011. b) Williams, TJ.; Chang, AY. Removable Protective Shell for Imaging Agents and Bioactive Substances. PCT Int. Appl. WO 2012178184 A2. 2012.
8. (a) Frankel AD, Pabo CO. Cell. 1988; 55:1189. [PubMed: 2849510] (b) Wender PA, Mitchell DJ, Pattabiraman K, Pelkey ET, Steinman L, Rothbard JB. Proc. Natl. Acad. Sci. U. S. A. 2000; 97:13003. [PubMed: 11087855] (c) Rothbard JB, Garlington S, Lin Q, Kirschberg T, Kreider E, McGrane PL, Wender PA, Khavari PA. Nature Med. 2000; 6:1253. [PubMed: 11062537] (d) Rothbard JB, Jessop TC, Lewis RS, Murray BA, Wender PA. J. Am. Chem. Soc. 2004; 126:9506. [PubMed: 15291531]
9. Siprashvili Z, Scholl FA, Oliver SF, Adams A, Contag CH, Wender PA, Khavari PA. Human Gene Therapy. 2003; 14:1225. [PubMed: 12952594]
10. Wu X, Boz E, Sirkis AM, Chang AY, Williams TJ. J. Fluorine Chem. 2012; 135:292.
11. a) Janjic JM, Srinivas M, Kadayakkara DKK, Ahrens ET. J. Am. Chem. Soc. 2008; 130:2832. [PubMed: 18266363] b) Du W, Nystrom AM, Zhang L, Powell KT, Li Y, Cheng C, Wickline SA, Wooley KL. Biomacromolecules. 2008; 9:2826. [PubMed: 18795785]
12. Diou O, Tsapis N, Fattal E. Expert Opin. Drug Deliv. 2012; 9:1475. [PubMed: 23092183]
13. Ruiz-Cabelloa J, Barnetta BP, Bottomleya PA, Bulte JWM. NMR Biomed. 2011; 24:114. [PubMed: 20842758]
14. Wallach, DFH.; Mathur, R. Handbook of Nonmedical Applications of Liposomes. Lasic, DD.; Barenholz, DDLY.; Barenholz, Y., editors. CRC Press; 1996. p. 115-123.
15. (a) Kotov SV, Ivanov GD, Kostov GK. J. Fluorine Chem. 1988; 41:293.(b) Tortelli V, Tonelli C. J. Fluorine Chem. 1990; 47:199.(c) Takakura T, Yamabe M, Kato M. J. Fluorine Chem. 1988; 41:173.
16. a) Kumar A, Zhang X, Liang X. Biotechnol. Adv. 2012 in press. b) Rana S, Bajaj A, Mout R, Rotello VM. Adv. Drug Delivery Rev. 2012; 64:200.c) Rippel RA, Seifalian AM. J. Nanosci. Nanotechnol. 2011; 11:3740. [PubMed: 21780364] d) Kim C, Ghosh P, Rotello VM. Nanoscale. 2009; 1:61. [PubMed: 20644861] e) Kumawat L, Jain A. Int. J. Pharm. Sci. Res. 2012; 3:52.
17. a) Gangwar RK, Dhumale VA, Kumari D, Nakate UT, Gosavi SW, Sharma RB, Kale SN, Datar S. Mat. Sci. Eng. C. 2012; 32:2659.b) Kodiyan A, Silva EA, Kim J, Aizenberg M, Mooney DJ. ACS Nano. 2012; 6:4796. [PubMed: 22650310]
18. a) Kennedy LC, Bear AS, Young JK, Lewinski NA, Kim J, Foster AE, Drezek RA. Nanoscale Res. Lett. 2011; 6:283. [PubMed: 21711861] b) Akiyama Y, Mori T, Katayama Y, Niidome T. J. Controlled Release. 2009; 139:81.c) Mirkin CA, Letsinger RL, Mucic RC, Storhoff JJ. Nature. 1996; 382:607. [PubMed: 8757129]
19. Weare WW, Reed SM, Warner MG, Hutchison JE. J. Am. Chem. Soc. 2000; 122:12890.
20. Warner MG, Reed SM, Hutchison JE. Chem. Mater. 2000; 12:3316.
21. Wallner A, Jafri SHM, Blom T, Gogoll A, Leifer K, Baumgartner J, Ottosson H. Langmuir. 2011; 27:9057. [PubMed: 21667939]
22. Mizukami S, Takikawa R, Sugihara F, Hori Y, Tochio H, Walchli M, Shirakawa M, Kiuchi K. J. Am. Chem. Soc. 2007; 130:794. [PubMed: 18154336]
23. Raghunand N, Jagadish B, Trouard TP, Galons JP, Gillies RJ, Mash EA. Magn. Reson. Med. 2006; 55:1272. [PubMed: 16700014]
24. (12-mercaptododecyl)phosphonic acid was purchased from SiKÉMIA.
25. Dichloromethane was purchased from Macron Chemicals.
26. Chloroauric acid was purchased from STREM Chemicals.
27. Triethylsilane was purchased from Alfa Aesar.

28. Ethanol was purchased from Koptec.

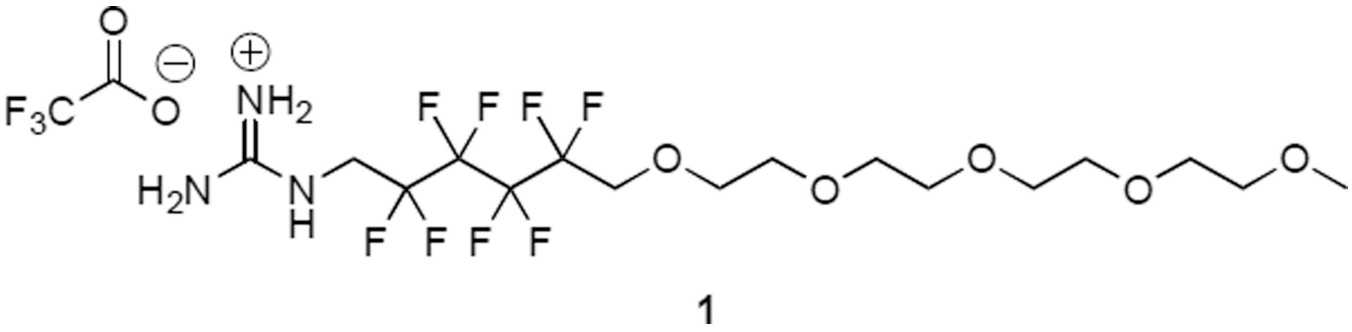

1

Fig. 1.
Structure of monomer **1**.

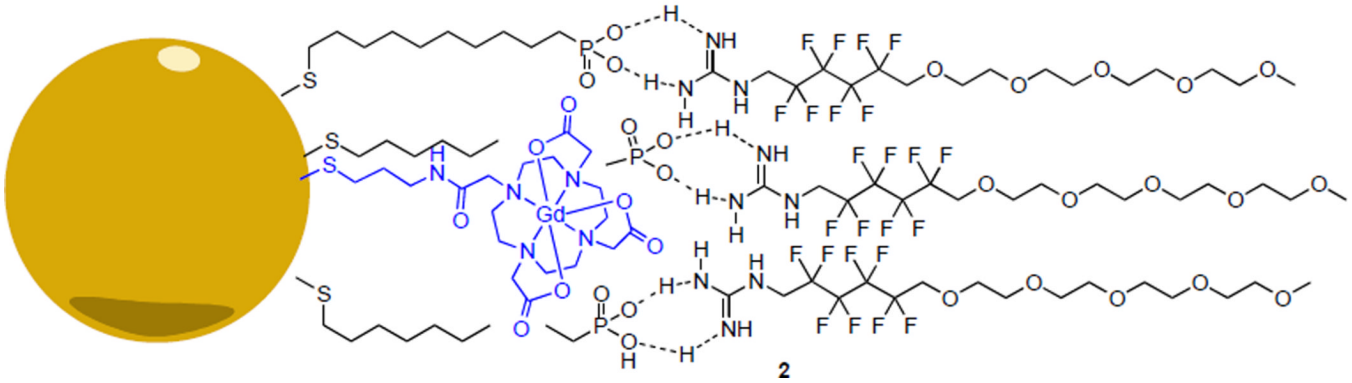

Fig. 2.
Hypothetical interactions between phosphonate core and guanidine shell to yield shell coated phosphonate particle **2**

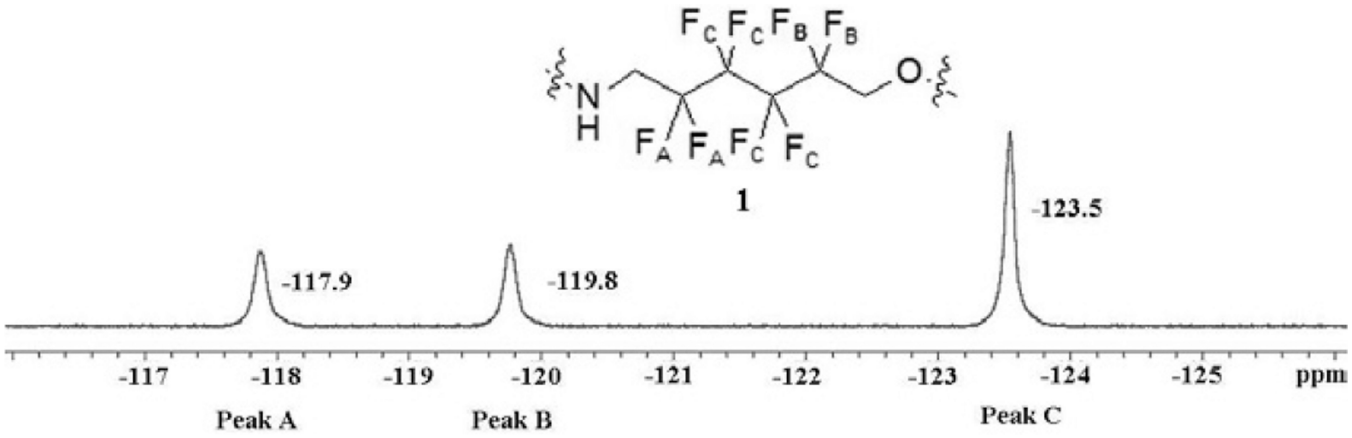

Fig. 3.
NMR Properties of **1**.

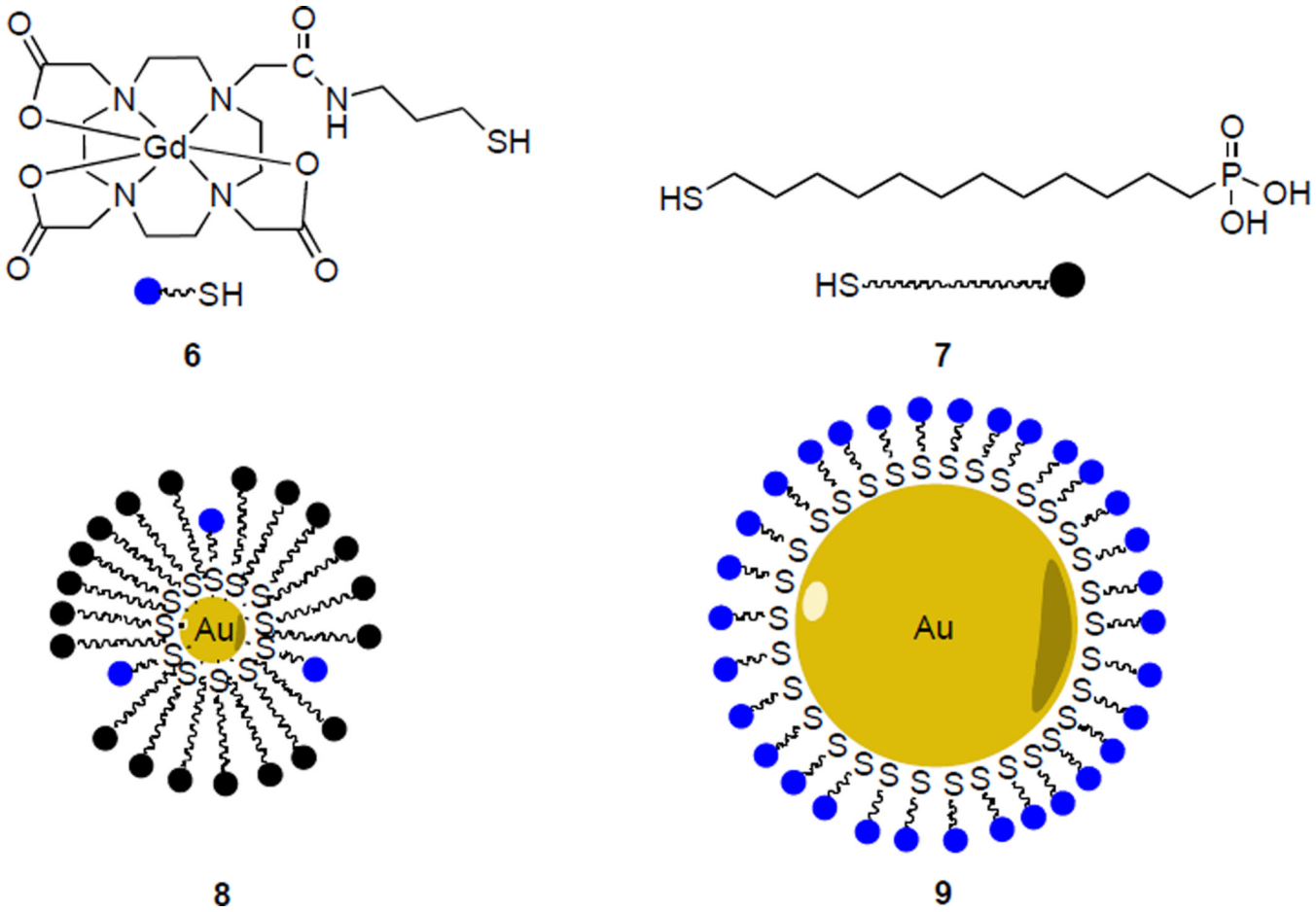

Fig. 4.
Composition of nanoparticles.

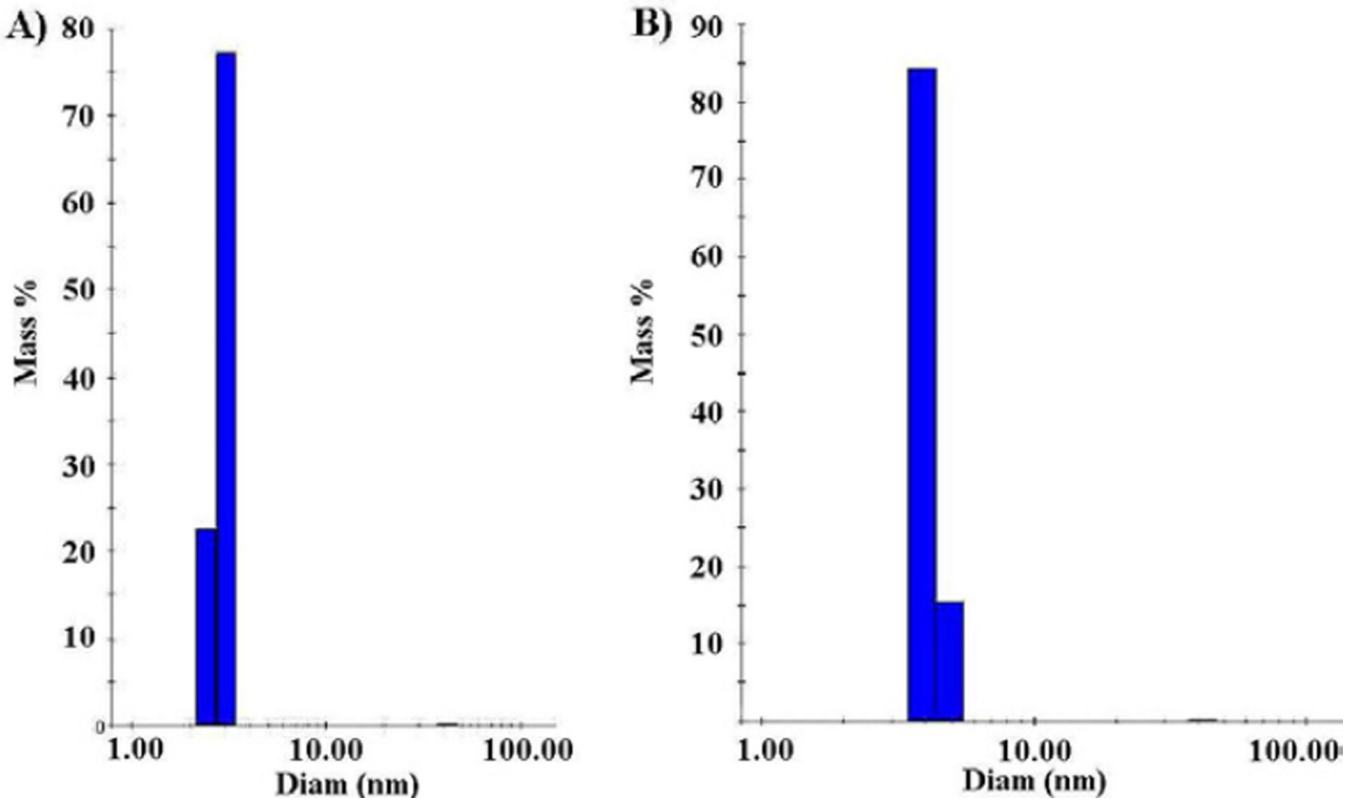

Fig. 5.

(A) DLS of particle **8** (average hydrodynamic diameter = 3.0 nm) (B) DLS of particle **2** (after the addition of monomer **1**, hydrodynamic diameter = 4.0 nm).

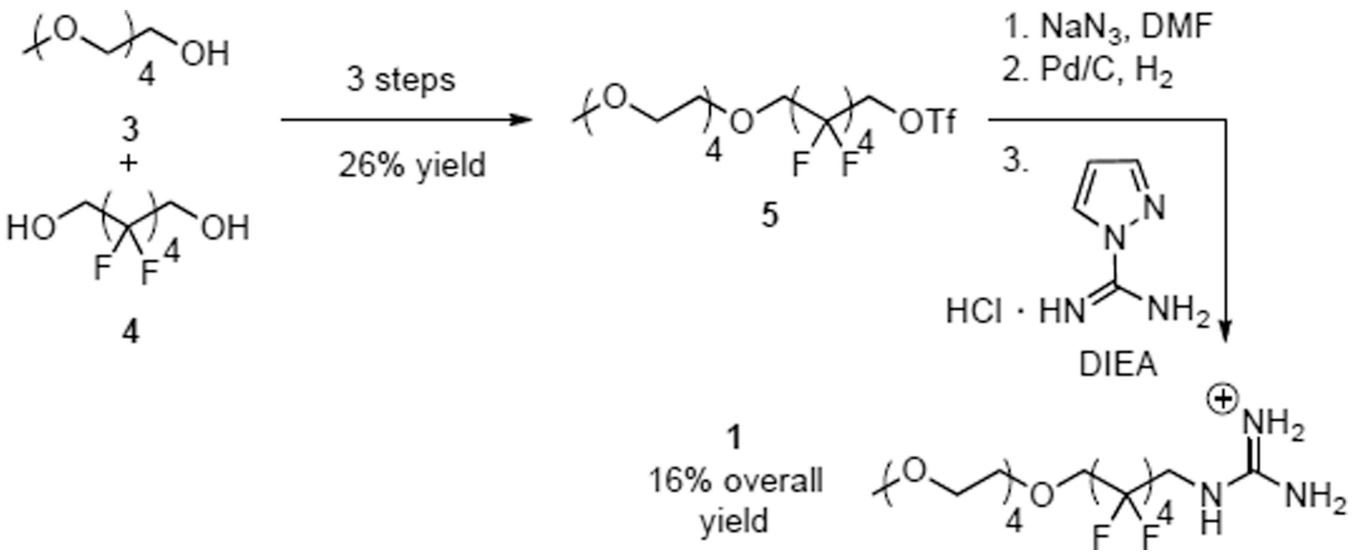

Scheme 1.
Synthesis of monomer **1**.

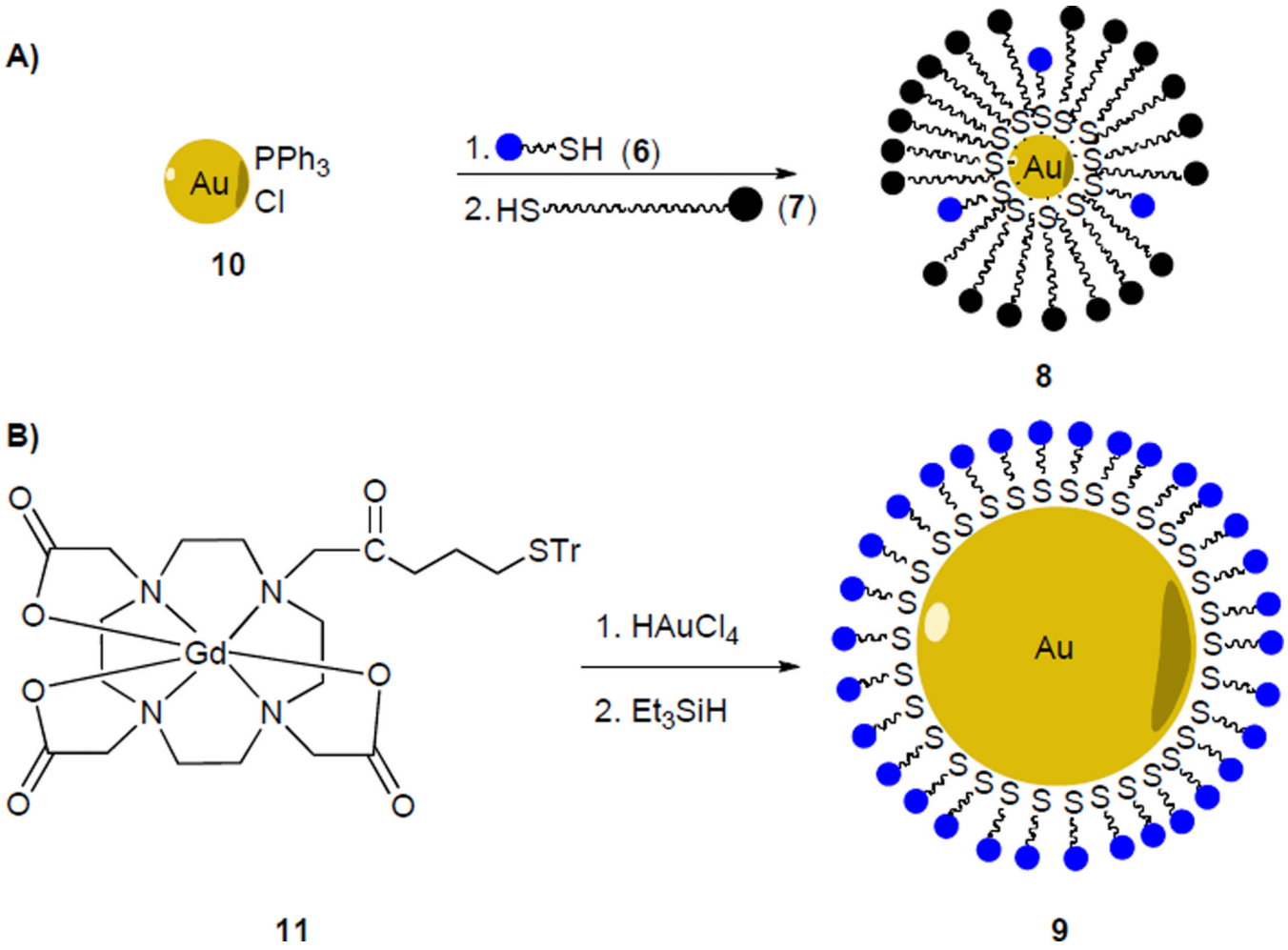

Scheme 2.
Synthesis of nanparticles.

Table 1

Decrease of ^{19}F T_1 when particle is added to **1**.

	Peak A −117.9 ppm	**Peak B −119.8 ppm**	**Peak C −123.5 ppm**
1	457(8) ms	436(7) ms	497(7) ms
1 + **8**	332(14) ms	348(4) ms	385(4) ms
1 + **9**	434(6) ms	431(7) ms	481(5) ms
1 + $GdCl_3$	429(13) ms	396(8) ms	466(6) ms